

National Aeronautics and Space Administration



TID Effects in Space-Like Variable Dose Rates

Richard D. Harris
Jet Propulsion Laboratory
Pasadena, California

Jet Propulsion Laboratory
California Institute of Technology
Pasadena, California

JPL Publication 08-17 4/08



TID Effects in Space-Like Variable Dose Rates

NASA Electronic Parts and Packaging (NEPP) Program
Office of Safety and Mission Assurance

Richard D. Harris
Jet Propulsion Laboratory
Pasadena, California

NASA WBS: 939904.01.11.30
JPL Project Number: 102197
Task Number: 3.31.7

Jet Propulsion Laboratory
4800 Oak Grove Drive
Pasadena, CA 91109

<http://nepp.nasa.gov>

This research was carried out at the Jet Propulsion Laboratory, California Institute of Technology, and was sponsored by the National Aeronautics and Space Administration Electronic Parts and Packaging (NEPP) Program.

Reference herein to any specific commercial product, process, or service by trade name, trademark, manufacturer, or otherwise, does not constitute or imply its endorsement by the United States Government or the Jet Propulsion Laboratory, California Institute of Technology.

Copyright 2008. California Institute of Technology. Government sponsorship acknowledged.

TID Effects in Space-Like Variable Dose Rates

Richard D. Harris

NEPP Program

Office of Safety & Mission Assurance

WBS 939904.01.11.30 under TASK ORDER NMO7-10824

Project Number: 102197

Task Number: 3.31.7

3/14/2008

PI: Richard D. Harris

Abstract—The degradation of the LM193 dual voltage comparator has been studied with different types of TID dose rates. These include several different constant dose rates and a variable dose rate that simulates the behavior of a solar flare. The varying dose rate of a solar flare is the type of real total dose exposure that a space mission might see in lunar or Martian orbit. A comparison of these types of dose rates is made to explore how well the constant dose rates used for typical part testing predicts the performance during a simulated space-like mission.

Table of Contents

SECTIONS

Abstract.....	1
1.0 Introduction	3
2.0 Solar Flare Analysis	3
3.0 Experimental Procedure	5
4.0 Experimental Results.....	6
5.0 Discussion and Analysis.....	7
6.0 Conclusions	8
7.0 Recommendations for Future Work.....	9
8.0 Acknowledgement.....	9
9.0 References	10

FIGURES

1 Solar proton flux for the October 1989 “Halloween” flare.....	4
2 Actual total dose rate vs. time for the Halloween flare and the simulated dose rate schedule.....	4
3 Actual accumulated total dose vs. time for the Halloween flare and the simulated accumulated dose schedule.....	5
4 The modified simulated dose rate schedule for the Co-60 irradiation and the actual schedule as delivered to the parts.....	6
5 Degradation of $+I_B$ vs. dose for the various dose rate conditions; both constant and variable.....	7
6 Degradation of $+I_B$ vs. dose for the simulated solar flare compared to two models.....	8

1.0 INTRODUCTION

Most enhanced low dose rate sensitivity (ELDRS) testing on linear bipolar parts has been performed using Co-60 sources with a constant dose rate, comparing degradation following high dose rate (HDR, typically ~ 50 rad(Si)/s) exposure with those following low dose rate (LDR, typically ~ 0.005 – 0.01 rad(Si)/s) exposure [1]. However, most space missions do not see constant dose rates, but rather dose rates that vary throughout the mission profile. Examples include lunar or Martian missions where the dose rates are low except during solar flares when the dose rates are orders of magnitude larger.

Previous work has shown that for parts that experience ELDRS, the degradation rate increases as the dose rate gets lower [2]. For some parts, there does not appear to be a worst case dose rate, or it is so low that it is not practical to perform total ionizing dose (TID) testing in a reasonable amount of time at that rate. For this reason, hardness assurance methodology has been the subject of many investigations and many accelerated test methods have been proposed [3, 4].

The present study was undertaken to compare the degradation observed in a real variable dose rate profile with the constant dose rates used in most testing regimens. The dose profile of a real solar flare was chosen to provide the alternating dose rate example; in this case the October 1989 “Halloween” flare. The LM193 dual voltage comparator from National Semiconductor was chosen as a representative part as previous work at JPL has shown it to have a strong ELDRS effect [5].

2.0 SOLAR FLARE ANALYSIS

The October 1989 “Halloween” flare was used as a representative solar flare. The solar proton flux is publically available from the National Oceanic and Atmospheric Administration (NOAA) Geostationary Operational Environmental Satellite (GOES) website [6]. The published proton flux *vs.* time is shown in Fig. 1 for this flare. There is quite a bit of interesting structure in the flux as the flare progresses through the days. The time period shown in Fig. 1 covers 12 days, with the first \sim half day being before the flare actually begins.

The total dose rate for each time segment was calculated from the proton flux data using the charged particle radiation transport tool NOVICE [7]. This is calculated as the dose rate behind 100 mils of aluminum (Al) shielding, a common baseline for environmental estimates at JPL. The total dose as calculated from this procedure is shown in Fig. 2 as the dose rate *vs.* time and in Fig. 3 as the total accumulated dose *vs.* time; in both cases, in blue. The time before the flare began, which we define as a dose rate of $\sim 1 \times 10^{-4}$ rad(Si)/s, is removed from the data in these figures. The calculated value of the background dose rate before the flare, not shown, is approximately 1×10^{-6} rad(Si)/s. This background value is actually an upper limit on the background as the background flux values in Fig. 1 represent instrument sensitivity limits, and not real measured values. As a result, the maximum dose rate during the flare, as seen in Fig. 2, exceeds the background by at least 5 orders of magnitude.

The continuously varying dose rate shown in Fig. 2 is not very practical to implement in the laboratory and so an approximate simulated dose rate schedule was developed from the actual dose rate data. This simulated schedule is depicted in Fig. 2 in red, and steps between the three different dose rates of 0.001, 0.01, and 0.1 rad(Si)/s. This schedule is a good approximation to

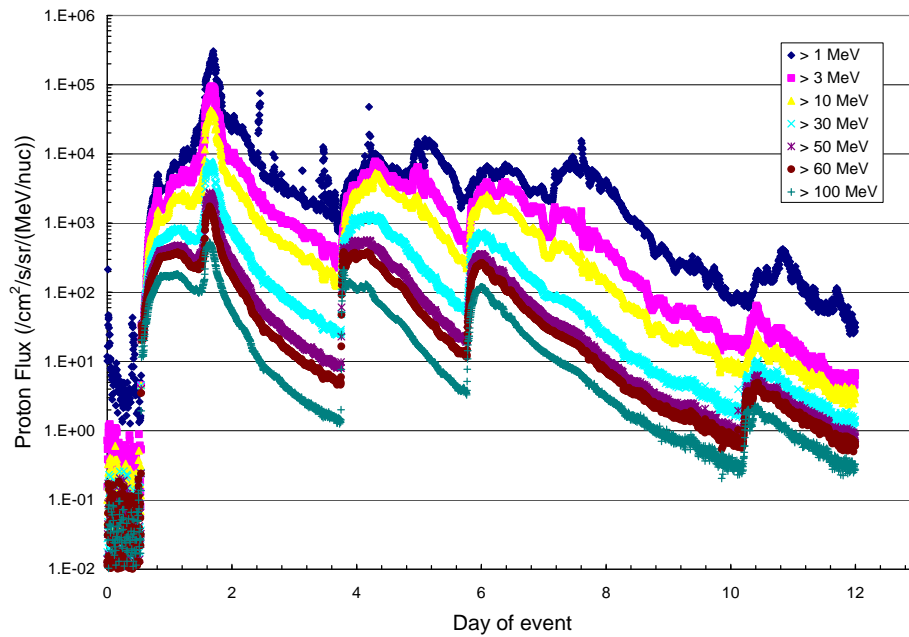


Figure 1. Solar proton flux for the October 1989 “Halloween” flare.

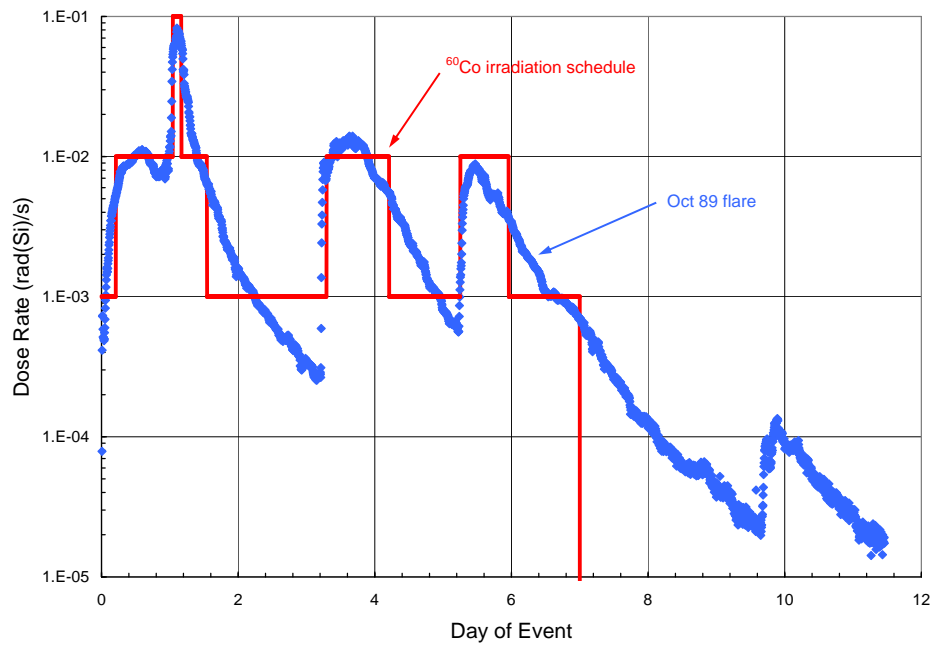


Figure 2. Actual total dose rate vs. time for the Halloween flare (in blue) and the simulated dose rate schedule (in red). Dose rate is calculated as that behind 100 mils of Al shielding.

the actual dose rate and also to the total accumulated dose as seen in Fig. 3. Based on the rapidly decreasing dose rate of Fig. 2, the simulated schedule was defined to be complete after 7 days. This gave a total accumulated simulated dose of 3.88 krad(Si) compared to actual total dose of 3.87 krad(Si) as depicted in Fig. 3.

3.0 EXPERIMENTAL PROCEDURE

The device used to compare the degradation under the different dose rate conditions was the LM193 dual voltage comparator from National Semiconductor. The part number for the device tested is LM193J/883, where the J indicates that the part is packaged in an 8-pin cerdip. The lot date code for the parts evaluated in this study was 0608. This part choice was made based on previous studies at JPL that showed that this part has a strong ELDRS effect [5]. (It should be noted that this date code precedes the recent announcement of the release of an ELDRS-free LM193 from National Semiconductor.)

Parts were irradiated in the JPL HDR and LDR Co-60 facilities at different dose rates as discussed below. Lead/aluminum (Pb/Al) shields covered the parts during irradiation in accordance with MIL-STD 883, Method 1019.7 [1]. In all cases, the parts were irradiated in an unbiased state (i.e., with the leads shorted together and grounded) as the previous studies at JPL showed that this bias condition produced the largest ELDRS effect [5]. Four parts were used for each dose rate condition to allow for determination of statistical variability within the lot of purchased parts.

Measurements were performed prior to the irradiation and then at a variety of steps throughout the Co-60 irradiation using an LTS-2020 mixed signal test system. While a number

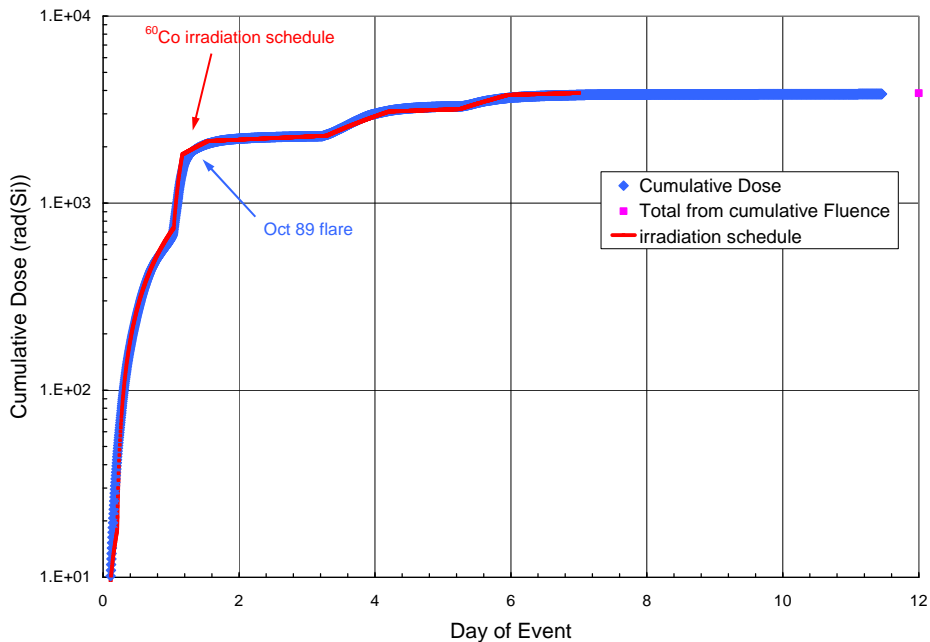


Figure 3. Actual accumulated total dose vs. time for the Halloween flare (in blue) and the simulated accumulated dose schedule (in red).

of parameters were measured at each step, the input bias current, $+I_B$, was singled out to monitor the degradation in this study.

The total accumulated dose from the flare and the simulated Co-60 schedule is 3.87 krad(Si). This total dose is a little on the low side to see a substantial amount of degradation at various steps along the way or at the end. Therefore, the simulated schedule shown in Fig. 2 was modified by doubling the dose rate in each step and doubling the length of each step. In this way, the total simulated accumulated dose was increased to 15.5 krad(Si) while keeping the spirit of the actual flare profile. The modified dose rate schedule is shown in Fig. 4, in red, along with the actual dose rate profile that the parts received, in black. The difference resulted from practical considerations on timing for measurements and dose rate changes.

The modified schedule called for irradiations at dose rates of 0.2, 0.02, and 0.002 rad(Si)/s. The JPL Co-60 irradiation facilities are both room irradiators. As such, it was possible to obtain each of these dose rates by placing the parts at the appropriate distance from the source. The 0.2 rad(Si)/s irradiation was performed in the HDR facility and the 0.02 and 0.002 rad(Si)/s irradiations were performed in the LDR facility. These positions were determined by use of an ion chamber dosimeter.

In addition to the variable dose rate schedule, parts were also irradiated at constant dose rate at each of the three different dose rates.

4.0 EXPERIMENTAL RESULTS

The degradation of $+I_B$ vs. dose for the various dose rate conditions is shown in Fig. 5. The data are plotted as the average of $\Delta +I_B$ for the four parts measured. The error bars represent

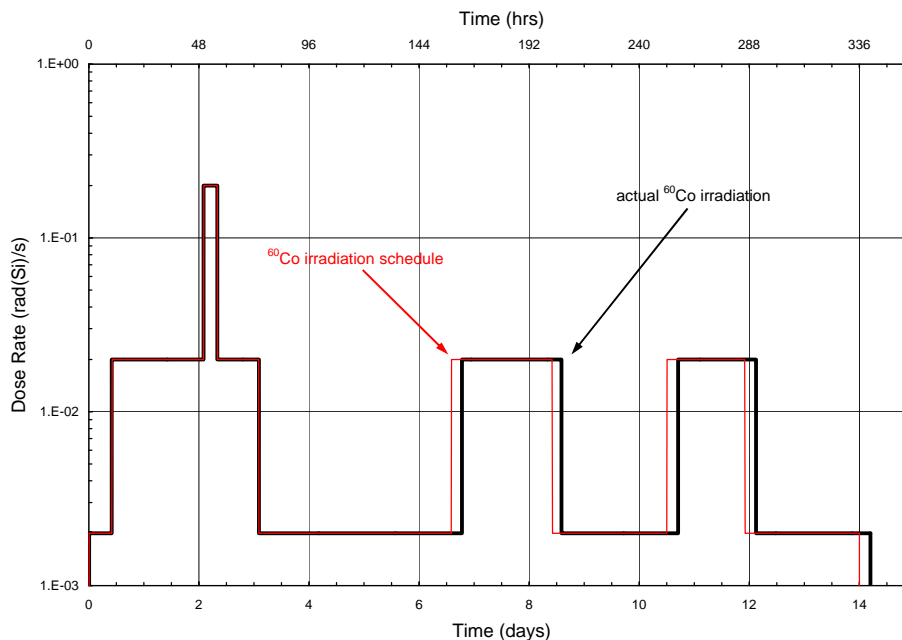


Figure 4. The modified simulated dose rate schedule for the Co-60 irradiation (in red) and the actual schedule as delivered to the parts (in black).

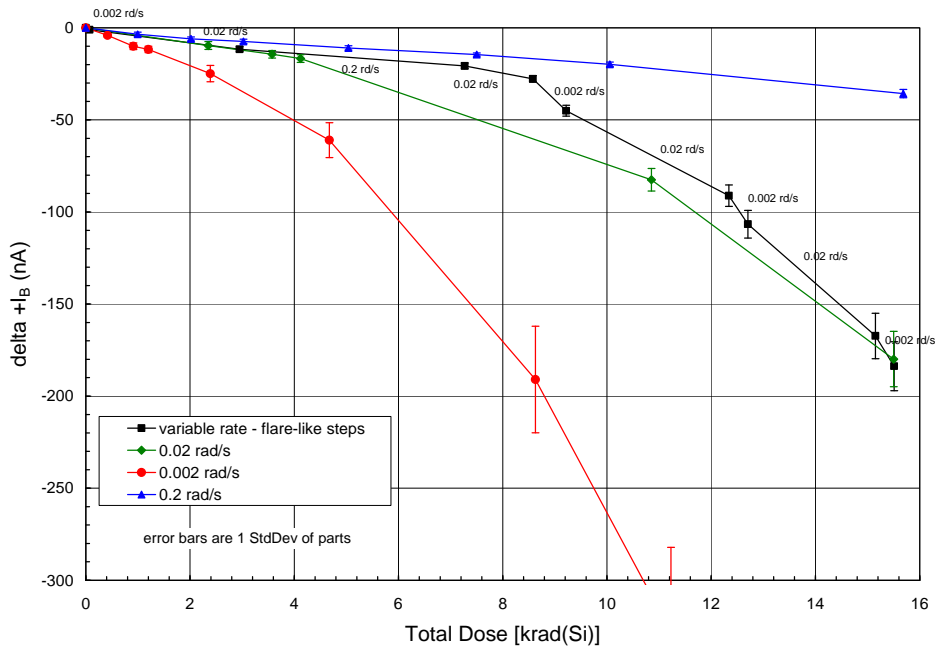


Figure 5. Degradation of $+I_B$ vs. dose for the various dose rate conditions; both constant and variable.

one standard deviation of the measured values of the four parts. Included in this figure are both the constant dose rate reference curves and the variable dose rate simulated solar flare curve.

The overall average dose rate during this irradiation schedule was 0.013 rad(Si)/s (15.5 krad over 14 days). As such, it was expected that the variable curve would lie between the constant 0.002 and 0.02 curves. However, as seen in Fig. 5, the curve exhibits on average somewhat less degradation than the 0.02 rad(Si)/s constant dose rate. This is considerably slower degradation than expected for the average dose rate. It is also very much slower than observed for the lowest constant dose rate of 0.002 rad(Si)/s. As a result, a typical strategy of trying to irradiate at, or near, the lowest dose that will be seen during the mission appears to produce a degradation curve that is very, very conservative.

Based on this single set of data, it appears that it may be possible to develop a good model for the amount of degradation expected by irradiating at a dose rate near the average mission dose rate rather than the lowest dose rate. This would be a big asset in estimating degradation in missions that expect very large dose levels. Before implementing such a concept, it will be necessary to test other mission profiles to see if the trend holds and to develop an accurate hardness assurance methodology.

5.0 DISCUSSION AND ANALYSIS

Two different models were tested to explain the shape of the degradation seen by the variable dose rate schedule. These are depicted in Fig. 6 along with the result of the variable rate irradiation. The first model is based on the assumption that the damage incurred in each dose rate step is a function of: 1) the amount of damage that has been accumulated up to that point, and 2) the dose rate in the step under consideration; i.e., how the sample got to the level of

degradation is not important. This was built up by taking the amount of degradation at the initial point of each step and finding the amount of dose required to give that amount of degradation at that dose rate. Then by adding the amount of dose in the step, the amount of degradation at the end of the step was determined. This was repeated for each step. The result is the red curve in Fig. 6. This model is the more intuitive of the two.

The second model was based on the assumption that the amount of degradation in each step is a function of: 1) the total amount of dose accumulated prior to the beginning of each step, and 2) the dose rate in that step. This model was built up by determining the additional amount of degradation that occurs at constant dose rate for the interval between the initial and final doses at that rate. These additional amounts were then summed to give the accumulated damage at each point. This is the blue curve in Fig. 6.

The two models bracket the experimental results as seen in Fig. 6. Both have the correct general shape, with changes in the slope for each of the steps. However, neither fits as well as was hoped. The degradation is not simply explained by a simple combination of the separate degradations in each of the various dose rates steps. Apparently, the part maintains some memory of how the previous degradation occurred; i.e. it remembers the previous dose rates.

6.0 CONCLUSIONS

Device degradation following constant TID dose rate exposure has been compared to that caused by a solar flare-like variable dose rate. Two different models are being developed to explain the behavior. The overall degradation rate of the variable dose rate is less than is expected based on an average dose rate during the variable event.

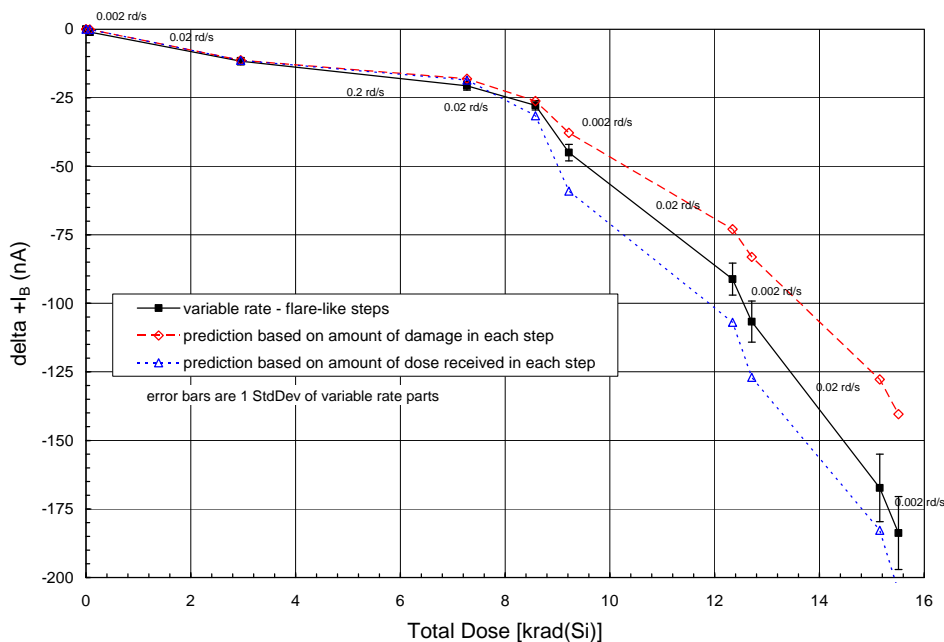


Figure 6. Degradation of $+I_B$ vs. dose for the simulated solar flare compared to two models. See text for discussion of the models.

7.0 RECOMMENDATIONS FOR FUTURE WORK

As a continuation of this work, there are four areas that could be addressed next.

- 1) The models developed during this task do not sufficiently explain the experimental results. While the correct general trends are seen in both models, the fits to the data are not as good as desired. Additional work needs to be performed to produce a better understanding and the better fit that would accompany it. It may be that a combination of the two models is the best solution.
- 2) The degradation curves shown in Fig. 5 are unusual for a plot of I_B degradation. It is generally expected that the degradation will be linear with dose [8]. It would be desirable to perform some spice simulations on the internal circuit of the LM193 to determine why the unexpected dependence is seen. It may be that this improved understanding of the internal LM193 circuitry would lend some insight into improving the models discussed above.
- 3) The amount of degradation seen for the LM193 under the simulated flare profile is less than would be expected if irradiated at the average dose rate and much less than expected if irradiated at the lowest dose rate in the profile. As suggested above, this has implications for hardness assurance methodology, particularly for missions with very high dose levels. To further explore this concept, it is desirable to extend this sort of experiment to other types of environments. A conversion of energetic particle flux to total dose has already been completed for several orbits of the upcoming Juno mission, which would be a good possibility for a second example.
- 4) Before applying the results of this study to hardness assurance methodology, additional part types need to be evaluated to determine the extent of variations between part types.

8.0 ACKNOWLEDGMENT

The solar flare proton flux data were located and converted to dose by Insoo Jun (Reliability Engineering Office, JPL) and Robin Evans (Reliability Engineering Office, JPL). The ability to simulate a solar flare would not have been possible without their contribution. Bernie Rax (Electric Parts Engineering Office, JPL) performed all the irradiations and part measurements. Helpful discussions about the LM193 and TID behavior were held with Steve McClure (Electric Parts Engineering Office, JPL) and Philippe Adell (Electric Parts Engineering Office, JPL).

9.0 REFERENCES

- [1] MIL-STD-883G, Method 1019.7, 2006.
- [2] A.H. Johnston, G.M. Swift, and B.G. Rax, "Total dose effects in conventional bipolar transistors and linear integrated circuits," *IEEE Trans. Nucl. Sci.*, vol. 41, no. 6, pp. 2427–2436, Dec. 1994.
- [3] R.L. Pease, M. Gehlhausen, J. Krieg, J. Titus, T. Turflinger, D. Emily, and L. Cohn, "Evaluation of proposed hardness assurance method for bipolar linear circuits with enhanced low dose rate sensitivity (ELDRS)," *IEEE Trans. Nucl. Sci.*, vol. 45, no. 6, pp. 2665–2672, Dec. 1998.
- [4] J. Boch, F. Saigne, R.D. Schrimpf, J.-R. Vaillie, L. Dusseau, S. Ducret, M. Bernard, E. Lorfevre, and C. Chatry, "Estimation of low-dose-rate degradation on bipolar linear integrated circuits using switching experiments," *Trans. Nucl. Sci.*, vol. 52, no. 6, pp. 2616–2621, Dec. 2005.
- [5] C.C. Yui, S.S. McClure, B.G. Rax, J.M. Lehman, T. D. Minto, M.D. Wiedeman, "Total Dose Bias Dependency and ELDRS Effects in Bipolar Linear Devices," 1997 IEEE Radiation Effects Data Workshop Record, pp. 131–137, 1997.
- [6] National Oceanic and Atmospheric Administration, National Geophysical Data Center. "SPIDR," Web site, 2008, <http://spidr.ngdc.noaa.gov/spidr/>
- [7] T. Jordan, "NOVICE, A Radiation Transport Shielding Code," Experimental and Mathematical Physics Consultants, Gaithersburg, MD, 2006.
- [8] A.H. Johnston, JPL, private communication.